Theoretical Investigations of NMR Chemical Shifts and Reactivities of Oxovanadium(v) Compounds

MICHAEL BÜHL,[1] FRED A. HAMPRECHT[2]

[1]*Organisch-Chemisches Institut, Universität Zürich, Winterthurerstr. 190, CH-8057 Zürich, Switzerland*

[2]*Department of Chemistry, ETH-Zentrum, Zürich, Switzerland*

Received 4 June 1997; accepted 9 June 1997

ABSTRACT: Employing gradient-corrected levels of density-functional theory (DFT), medium-sized basis sets, and optimized geometries, chemical shifts are calculated for $[VOCl_nF_{3-n}]$ ($n = 0$–3), VF_5, $[VO(OCH_2CH_2)_3N]$, $[V(CO)_6]^-$, $[V(CO)_5(N_2)]^-$, as well as for the model compounds $[VO(OMe)_nMe_{3-n}]$ ($n =$ 0–3) and their AlH_3 adducts. Experimental trends in $\delta(^{51}V)$ are well reproduced with DFT-based methods; for example, the slopes of the $\delta(^{51}V)_{calc}$ vs. $\delta(^{51}V)_{expt}$ linear regression lines are 0.92 and 1.03 at the GIAO-BP86 and GIAO-B3LYP levels, respectively. Ethylene polymerization observed with $[V(O\cdots AlX_3)(OR)_nR'_{3-n}]$ (X, R, R' = bulky alkyl, aryl, or silyl groups) is shown for model systems ($X = H$, $R = R' = Me$) to proceed by insertion of the olefin into a V—C bond via a transition state with approximate square-pyramidal coordination about vanadium. For the tri- and dialkyl derivatives ($n = 0, 1$), similar activation barriers of ca. 19 kcal/mol are computed (BP86 level including zero-point energies), whereas that of the monoalkyl species ($n = 2$) is predicted to be much higher, ca. 30 kcal/mol. The relevance of these results for the apparent relationship between $\delta(^{51}V)$ and catalytic activities is discussed.
 J. Comput Chem **19**: 113–122, 1998

Keywords: density-functional theory; ^{51}V; chemical shift calculations; mechanism of ethylene polymerization; barriers for ethylene insertion

Correspondence to: M. Bühl; e-mail: buehl@oci.unizh.ch

 CCC 0192-8651 / 98 / 020113-10

Introduction

Correlations of kinetic parameters and NMR chemical shifts are potentially very useful because quantities that are difficult to determine (e.g., rate constants) can be estimated from ones that are more easily accessible (via NMR spectroscopy). Even though there is no general, *a priori* relationship between these properties, a number of such correlations has been established empirically for transition-metal compounds.[1–7] For instance, chemical shifts of transition metals have been correlated with rate constants for certain insertion or substitution reactions.[1–5] We have become interested in the study of such relationships employing the tools of modern density-functional theory (DFT),[8,9] as these are well suited for describing reactivities[10] and chemical shifts[11–18] of transition-metal complexes. For instance, for $[Fe(CO)_2(C_5H_5)R]$ (R = Me, Bu, i-Pr), the computed Fe—C(alkyl) bond dissociation energy decreases as R becomes bulkier,[19] consistent with the trend observed for the rate constants for PPh_3-induced CO insertion into these bonds.[5] In the $[Rh(CO)_2(C_5H_4X)] + PH_3$ model system (X = H, Cl, NMe_2, NO_2), the computed trends in the activation barriers for CO/PH_3 substitution[20] parallel those of the experimental rate constants for CO/PPh_3 exchange.[2] Because the corresponding trends in both $\delta(^{57}Fe)$ and $\delta(^{103}Rh)$ are reasonably well reproduced at ''pure DFT'' levels,[19,20] and even better employing hybrid functionals,[21] these NMR/reactivity correlations can be rationalized (for the iron species) or qualitatively reproduced (for the rhodium system) theoretically.

Because of the paramount importance of transition-metal complexes in homogeneous catalysis,[22] similar correlations of chemical shifts and catalytic activities are particularly interesting. Only a few examples are presently known, such as pyridine synthesis catalyzed by cyclopentadienylcobalt species,[6] and CO_2 hydrogenation catalyzed by rhodium complexes containing chelating phosphines.[7] Recent results obtained for the oxovanadium(V) species **1**–**4** (Scheme 1),[23] studied as model systems for a larger vanadate,[24] have also been quite promising in this context: Upon addition of alkylaluminum reagents, these compounds are mildly active catalysts for the homogeneous polymerization of ethylene. With an increasing number of OR groups, that is, in going from **1** to **4**, the ^{51}V nucleus becomes more and more shielded; in the same sequence, the catalytic activity decreases.[23]

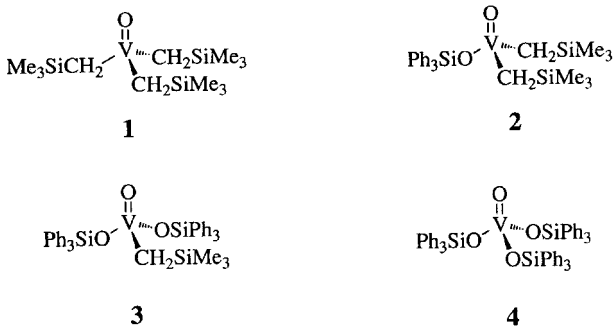

SCHEME 1.

To probe if this apparent relation is an ''intrinsic'' property of the potential energy surfaces (PESs) and electronic structures involved, we have now applied DFT methods to study the mechanism of ethylene polymerization for suitable model systems, calling special attention to the variation of the overall barrier with different substituents at the vanadium center. The calculations reveal remarkable stereoelectronic effects of alkoxy groups in the transition state, but no clear-cut trend in the barriers. In addition, DFT-computed $\delta(^{51}V)$ chemical shifts are reported and assessed for a larger set of vanadium compounds.

Computational Details

Geometries have been fully optimized without symmetry constraints (except where otherwise noted) employing the gradient-corrected exchange-correlation functionals of Becke (1988)[25] and Perdew (1986),[26] together with a fine integration grid (75 radial shells with 302 angular points per shell) and basis I; that is, Wachters's (14s11p6d)/[8s7p4d] all-electron basis augmented with one additional diffuse d and two 4p functions for V,[27,28] and standard 6-31G* basis set[29] for all other elements (denoted BP86/I). The nature of each stationary point, that is, minimum or transition state, has been established by frequency calculations. For the ''parent'' transition state **17(TS)** it has been ensured that the eigenvector corresponding to the imaginary frequency connects the desired minima by following the relevant part of the intrinsic reaction coordinate.[29] Unless otherwise noted, energies are reported at the BP86/I level including the BP86/I zero-point energies (ZPEs). All optimizations have been performed with the Gaussian-94 package.[30]

Magnetic shieldings have been computed with the GIAO (gauge-including atomic orbitals) DFT method as implemented in the Gaussian-94 program,[30,31] employing basis I and the BP86 combination of functionals, as well as Becke's three-parameter exchange DFT/Hartree–Fock hybrid functional[32] together with the correlation functional of Lee, Yang, and Parr (denoted B3LYP).[33] With the latter functional, calculations have also been performed employing the larger basis II, i.e. a well-tempered [14s11p8d] basis[34] on V (contracted from the 20s13p10d set and augmented with two additional p- and one additional d-shell of the well-tempered series) and IGLO basis II[35] for the ligands (which is essentially of polarized triple-zeta quality). In addition, computations have been carried out using the SOS-DFPT (sum-over-states density-functional perturbation theory) method[11,36] in its LOC1 approximation with the IGLO (individual gauge for localized orbitals) choice of gauge origins, as implemented in the deMon program,[37,38] employing the 1991 exchange-correlation functional of Perdew and Wang[39,40] together with a fine integration grid (FINE option) and basis II. Chemical shifts are reported relative to $[VOCl_3]$, the experimental standard, with computed absolute shieldings of −1959 (BP86/I), −2317 (B3LYP/I), −2418 (B3LYP/II), and −2010 ppm (SOS-DFPT/II).

Results and Discussion

CHEMICAL SHIFTS

^{51}V chemical shifts had been among the first applications of the SOS-DFPT method,[36] but only a few data have been reported. We employed a somewhat larger set of molecules which is displayed in Figure 1. In those cases where experimental geometries are known (**5**,[41,42] **8**,[43] **9**,[44] **10**,[45] **11**[46]), the BP86-optimized bond lengths tend to be slightly overestimated, as frequently encountered with these types of molecules.[47] Chemical shifts relative to **5**, the experimental standard, have been computed employing several density functionals and basis sets, and are shown in Table I. Experimental $\delta(^{51}V)$ values are known for **6**–**12**,[48,49] whereas **13**–**20** serve as model compounds for species with bulkier rests (analogous to **1**–**4**, but with OtBu instead of $OSiPh_3$ groups).[23] Because ^{51}V chemical shifts can be quite sensitive to effects of next-nearest neighbors, a direct comparison with experiment may be difficult for **13**–**20**. However, $\delta(^{51}V)$ values can also depend noticeably on concentration and solvent.[48,49] These effects are not accounted for in the calculations and may well be of the same order of magnitude as those of remote substituents. Perfect agreement between computed and experimental data can thus not be expected and it seems sensible to discuss and assess the trends of **5**–**20** together.

According to the slopes of $\delta(^{51}V)_{calc}$ vs. $\delta(^{51}V)_{exp}$ correlations in Table I, the ''pure DFT'' methods, SOS-DFPT and GIAO-BP86, underestimate substituent effects on ^{51}V chemical shifts somewhat (the slopes are smaller than unity, ca. 0.9). The same has been found at pure DFT levels for ^{103}Rh and, to a much larger extent, for ^{57}Fe chemical shifts.[19,20] Whereas the chemical shift ranges of the latter two nuclei are very well described with the hybrid B3LYP functional (with slopes close to unity), substituent effects on $\delta(^{51}V)$ appear to be slightly overestimated with this functional: the $\delta(^{51}V)_{calc}$ vs. $\delta(^{51}V)_{exp}$ slope is 1.03 and 1.06 employing basis I and II, respectively; that is, somewhat larger than unity. Nevertheless, the trends in $\delta(^{51}V)$ are well reproduced over the whole chemical shift range covered (ca. 3500 ppm). The mean absolute difference between computed and experimental data, 110 ppm (GIAO-B3LYP, Table I) or ca. 3% of the shift range, should be considered excellent in view of the aforementioned limitations. This is also apparent from the graphical representations of the GIAO-BP86 and B3LYP results in Figure 2. It is also noteworthy that basis-set effects appear to be relatively small in most cases (compare GIAO-B3LYP/I and B3LYP/II entries in Table I).

One trend is of special interest for the purpose of this study, namely that of successively replacing alkyl groups by alkoxy rests in going from the model systems **13** to **16** or from **17** to **20**. In both sequences, the GIAO-B3LYP data show variations very similar to those observed for the bulkier derivatives, with $\Delta\delta(^{51}V)$ ''increments'' per alkoxy substitution ranging from ca. −420 to −890 ppm (GIAO-B3LYP/II), compared to −470 to −870 ppm (experiment, see Table I). Likewise, the changes in $\delta(^{51}V)$ upon AlX_3 complex formation are reproduced, at least qualitatively, at the GIAO-B3LYP level (see Table II). The corresponding experimental data have—in conjunction with $\delta(^{17}O)$ measurements—led to the conclusion that the alkylaluminum reagents are coordinated to the V=O oxygen atom.[23] This conclusion is fully

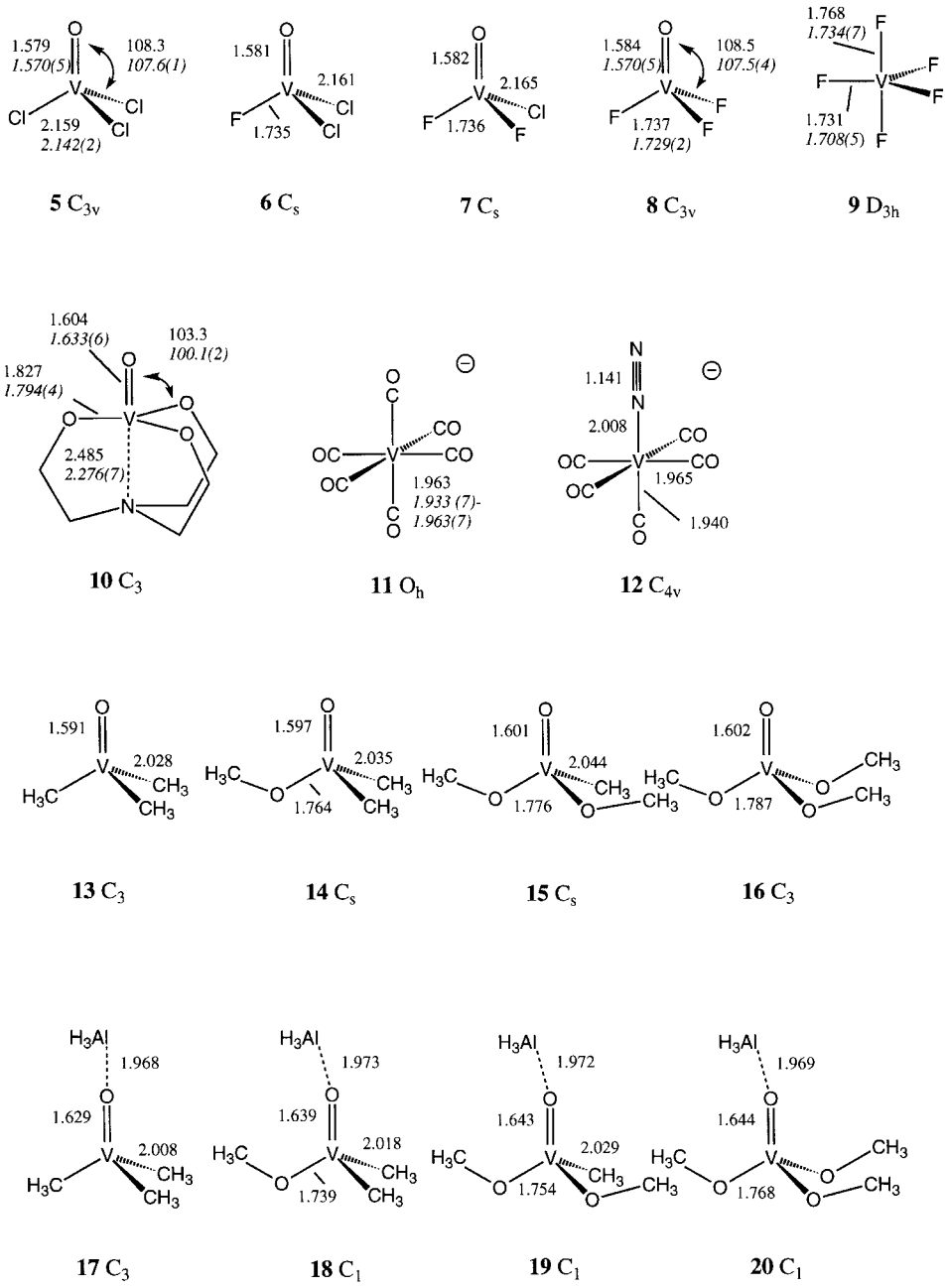

FIGURE 1. Vanadium compounds of this study. Key geometrical parameters optimized at the BP86 / I level are included, as are experimental data, where available.

supported by the structure and chemical shift calculations reported here.

The IGLO method allows a breakdown of the total shift into contributions from localized MOs which can help to rationalize the trends in the model systems **13**–**20** (see the key contributions from the valence shell in Table III). Not surprisingly, the largest part of the $\Delta\delta(^{51}V)$ alkoxy-substitution increments arises from the difference in V—C vs. V—O contributions [compare Σ(V—X) in going from **13** to **16** or from **17** to **20**, Table III]. V—C bonds are weaker than V—O bonds, resulting in a reduced energetic separation of the corresponding occupied and virtual MOs and, thus,

TABLE I.
DFT-Calculated ^{51}V Chemical Shifts (in ppm Relative to 5).[a]

Molecule	SOS-DFPT / II	BP86 / I	B3LYP / I	B3LYP / II	Experiment[b]
5[$VOCl_3$]	0	0	0	0	0
6[$VOCl_2F$]	−234	−243	−313	−312	−341
7[$VOClF_2$]	−484	−490	−621	−621	−582
8[VOF_3]	−710	−727	−909	−914	−757
9[VF_5]	−646	−678	−937	−945	−895
10[$VO(OCH_2CH_2)_3N$]	−298	−321	−477	−474	−380
11[$V(CO)_6]^-$	−2090	−2064	−2298	−2350	−1952
12[$V(CO)_5(N_2)]^-$	−1847	−1842	−2048	−2096	−1671
13[$VOMe_3$]	818	1048	1062	1097	1205
14[$VO(OMe)Me_2$]	271	405	348	364	470
15[$VO(OMe)_2Me$]	−213	−180	−291	−284	−210
16[$VO(OMe)_3$]	−501	−536	−703	−702	−676
17[$V(=OAlH_3)Me_3$]	1080	1335	1407	1453	1575
18[$V(=OAlH_3)(OMe)Me_2$]	427	571	540	559	727
19[$V(=OAlH_3)(OMe)_2Me$]	−140	−104	−214	−209	−143
20[$V(=OAlH_3)(OMe)_3$]	−492	−519	−712	−716	−742
Slope[c]	0.87	0.92	1.03	1.06	
Intercept[c]	−83	0	−104	−96	
Mean absolute deviation from expt.	169	114	119	118	

[a] BP86 / I geometries employed.
[b] For **5**–**12**, from refs. 48, 49; for **13**–**20**, data for CH_2SiMe_3 / OtBu derivatives from ref. 23.
[c] From $\delta(^{51}V)_{calc}$ vs. $\delta(^{51}V)_{exp}$ linear regressions.

in larger paramagnetic contributions, consistent with the π-donor capabilities of the oxygen substituent. Upon AlH_3 coordination, both V—C and V—O contributions become more negative, that is, more paramagnetic [compare Σ(V—X) in going from **13** to **17** or from **16** to **20**, Table III]. At the same time, the contributions from the terminal oxygen atom [Σ(V=O) in Table III] become less paramagnetic. The relative magnitude of these changes are such that a net deshielding and a net shielding is produced for **13** and **16**, respectively, reflecting the trend in the experimental chemical shifts.[50]

ETHYLENE POLYMERIZATION

As pointed out above, the experimental trends in $\delta(^{51}V)$ for the alkyl aluminum adducts of **1**–**4** (which are very similar to those of the OtBu derivatives given in Table I) can be well reproduced with DFT methods for the model systems **17**–**20**. How well are the reactivities toward ethylene described? No detailed kinetic studies have been performed, but from the yields of polyethylene under identical reaction conditions (950, 840, 225, and 183 mg for the alkylaluminum adducts of **1**, **2**, **3**, and **4**, respectively)[23] it appears that the catalytic activity decreases as more oxygen donors are introduced. A plausible mechanism for the polymerization reaction is the insertion of ethylene into a V—C bond. The catalyst derived from **4** has no such V—C bonds and it has been suspected that its (low) activity actually arises from traces of **3** that are produced under the reaction conditions.[23] The question is, what rate-determining barriers are computed for the catalytic cycle involving the model compounds **17**, **18**, and **19**, and can these barriers be related to the observed catalytic activities?

First, we consider ethylene insertion into the trimethyl derivative **17**. The stationary points on the BP86/I PES are depicted in Figure 3. The most striking structural feature of the transition state **17(TS)** is the coordination geometry about the vanadium atom which can be described as approximately square pyramidal (counting the carbon atoms of the forming and breaking V—C bonds as coordination sites). The increase in coordination number from 4 (**17**) to 5 (**17(TS)**) is similar to that from, for example, [VOF_3] to the well-known [$VOF_4]^-$.[51] No minimum corresponding to a "π-complex" prior to insertion could be located. For other olefin-polymerizing systems such as [MX_2—$CH_3]^+$ (M = Ti, Zr; X = Cl, C_5H_5),[52–55] π-complexes have been found to be more stable

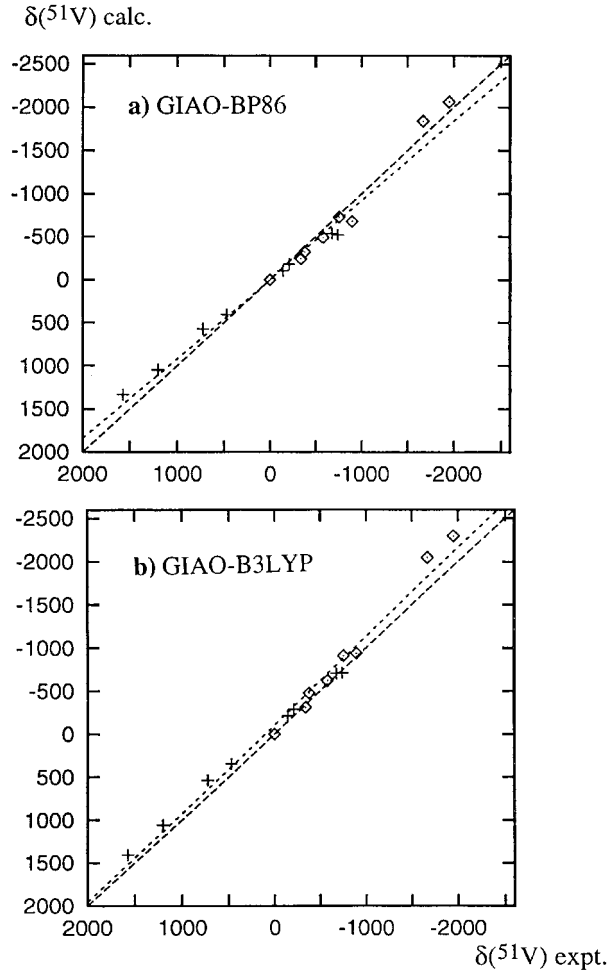

FIGURE 2. Plot of computed vs. experimental ^{51}V chemical shifts employing basis I and (a) GIAO-BP86 or (b) BIAO-B3LYP methods. (◇) Compounds **5**–**12**; (+) model systems **13**–**20**. Linear regression lines (dotted) and ideal lines with the slope = 1 (dashed) are included.

than the reactants, in some cases with very low barriers for subsequent insertion (for $[Zr(C_5H_5)_2CH_3]^+$, for instance, the barrier is so low that insertion is probably not the rate-determining step). Compared to the metal atoms in $[MX_2CH_3]^+$, however, the vanadium center in **17** is coordinatively more saturated and the reaction has a notable activation energy: at the BP86/I + ZPE level, the insertion barrier is 19.1 kcal/mol. This value appears somewhat large, but may still be overcome under experimental conditions (room temperature and elevated pressures).

As expected, the formation of the product **21** has a substantial driving force, −22.0 kcal/mol, which is essentially that of converting C—C π to σ bonds (cf. the $CH_3—CH_3 + CH_2=CH_2 \rightarrow CH_3—CH_2—CH_2—CH_3$ reaction, −22.7 kcal/mol at the same level). The gauche conformation of **21** shown in Figure 3 is isoenergetic with the trans isomer. The next ethylene molecule may be inserted into the V—C(propyl) bond, presumably with a similar barrier as into the V—C(methyl) bond, and so on, eventually producing polyethylene.

Now we turn to the effect on the insertion barrier of oxygen donors bound to vanadium, first in going from **17** to the monomethoxy system **18**. Because the transition state **17(TS)** has no symmetry, in principle all three methyl groups could be replaced by methoxy affording three different transition structures. Indeed, all of these are true transition states at the BP86/I level and are displayed in Figure 4. The first one, **18(TSb)**, corresponds to the insertion into the V—O bond of **18**. As V—O bonds are stronger then V—C bonds,[56] insertion into the former is expected to take place less easily. Accordingly, a large barrier is computed for this process via **18(TSb)**, ca. 31 kcal/mol. It is probably safe to assume that the corresponding barrier for the trialkoxy derivatives will be similarly high and that the pure catalyst derived from **4** would indeed be inactive at ambient temperature, as has been suspected.[23]

The other two structures in Figure 4, **18(TSa)** and **18(TS)**, are transition states for insertion of ethylene into a V—C bond, eventually leading to the same product. The difference between the two is that the methoxy rest is trans to the leaving methyl group in **18(TSa)** and cis in **18(TS)**. Quite surprisingly, there is a large energetic difference between both: **18(TSa)** is computed to be higher in energy than **18(TS)** by more than 6 kcal/mol. The

TABLE II.
Changes $\Delta\delta(^{51}V)$ of $[VO(OR)_nR'_{3-n}]$ upon Complex Formation with AlX_3.

Molecules	SOS-DFPT / II	B3LYP / II[a]	Expt.[b]
13 → **17**	+262	+356	+370
14 → **18**	+166	+195	+257
15 → **19**	+76	+75	+67
16 → **20**	+9	−14	−66

[a] R, R' = Me, X = H.
[b] X, R' = CH_2SiMe_3 and R = tBu, from ref. 23.

TABLE III.
LMO Contributions from Valence Shell to ^{51}V Magnetic Shielding, SOS-DFPT-IGLO / II Level.

Molecule	σ(V)[a]	Σ(V=O)[b]	Σ(V—X)[c]
13	−2828	−1194	−3192
16	−1509	−1291	−1782
17	−3090	−934	−3543
20	−1518	−1014	−1956

[a]Absolute shielding of the vanadium nucleus (with respect to the bare nucleus); note the different sign convention as compared to chemical shifts δ: for σ, negative values denote deshielding.
[b]Sum of all contributions associated with the terminal oxygen atom (including lone pairs or O—Al bonds).
[c]Sum of all contributions associated with the V—C bonds or with the ''singly bonded'' oxygen atoms (including lone pairs).

methoxy group thus exerts a pronounced stereoelectronic effect in the transition state. Apparently, there is a destabilizing effect on the leaving methyl group in **18(TSa)**, which can be seen from the ca. 0.1-Å elongation of the breaking V—C bond with respect to that in **18a(TS)** (see Fig. 4). Hence, the preferred pathway should proceed via **18(TS)**, requiring a similar activation as **17**. Incidentally, the barrier for **18** is slightly higher than that for **17**, by 0.3 kcal/mol, consistent with the somewhat reduced catalytic activity observed in going from the system involving **1** to that involving **2**.[23]

Finally, for the dialkoxy compound **19** there is only one possible transition state for ethylene insertion into a V—C bond, **19(TS)**, which is shown in Figure 5. From the above results for **18(TS)** vs. **18(TSa)** and noting that **19(TS)** must have one methoxy group trans to the leaving methyl, an increase in the barrier can be anticipated for **19**. Indeed, the barrier computed for **19** is higher than that for **18**, but the magnitude of this increase is remarkable: a barrier of 30.2 kcal/mol is computed, clearly too high to be overcome at room temperature. This result is at variance with the activity observed with the catalyst derived from **3**.[23] More detailed experimental investigations are desirable, in particular to address the question if—in analogy to **4**—catalysis with **3** could also

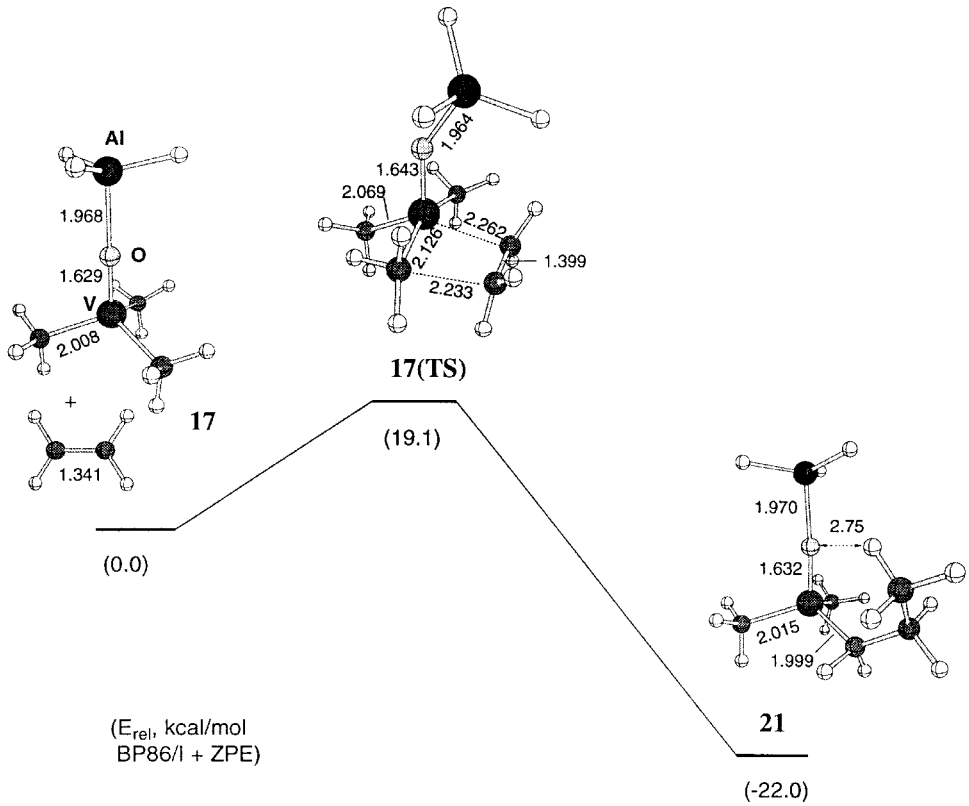

FIGURE 3. Schematic reaction profile of ethylene insertion into a V—C bond of **17**, including key distances from BP86 / I optimizations.

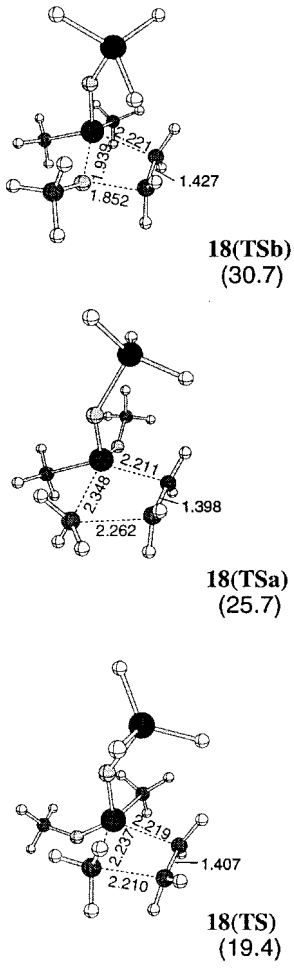

FIGURE 4. Transition states for ethylene insertion starting from **18**; relative energies with respect to **18** + ethylene are given in parentheses (kilocalories per mole BP86 / I + ZPE level).

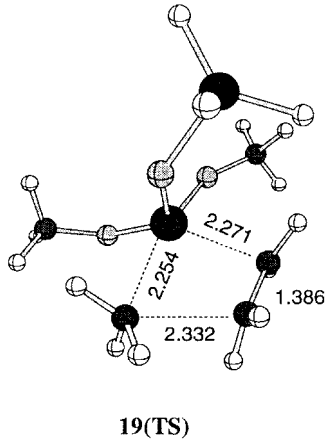

FIGURE 5. Transition state for ethylene insertion into the V—C bond of **19**, BP86 / I optimized.

arise from traces of **2** which might similarly be produced under the reaction conditions.

In any case, the results suggest that, in the $[VO(OMe)_nMe_{3-n}]$ system, and probably for other substituents as well, there should be no general, intrinsic relation between $\delta(^{51}V)$ and the barrier for ethylene polymerization. This conclusion is evident from the results for **18(TS)** and **18(TSa)** in Figure 4: The barrier is significantly influenced by stereoelectronic effects which are absent in the minimum. When the substituents at the vanadium center are varied, no strictly parallel effects on both $\delta(^{51}V)$ values and insertion barriers can thus be expected.

Conclusions

Experimental ^{51}V chemical shifts of a number of vanadium carbonyl and oxovanadium(V) complexes can be reproduced satisfactorily by employing DFT-based methods and medium-sized basis sets, even when calculations are performed for model compounds with less bulky groups than present in the actual systems. Substituent effects on $\delta(^{51}V)$ seem to be somewhat underestimated at pure DFT levels, and slightly overestimated employing hybrid functionals, but trends are generally described very well. For instance, variations in $\delta(^{51}V)$ of oxovanadium(V) compounds upon addition of alkylaluminum reagents are qualitatively recovered, confirming the conclusions drawn from the NMR spectra that stable Lewis-acid adducts are formed.

Ethylene polymerization by such adducts is shown for model systems to proceed by insertion of the olefin into V—C bonds via a square-pyramidal transition state. The computed barrier heights depend not only on the nature of the other substituents at vanadium (i.e., methyl or methoxy groups in this study) but also on their relative positions in the transition state. Because such stereoelectronic effects are absent in the minima, it appears that the observed, parallel trends in ^{51}V chemical shifts and catalytic activities of species derived from compounds **1**–**3** are not the result of an intrinsic relationship between these properties. Further calculations are in progress to identify systems with greater promise for such a relationship.

Acknowledgments

We thank Prof. Dr. W. Thiel for his support and interest. Calculations have been carried out on a Silicon Graphics PowerChallenge (Organisch-chemisches Institut, Universität Zürich) and on IBM RS6000 workstations (C4 cluster, ETH Zürich), as well as on a NEC-SX4 (CSCS, Manno, Switzerland).

References

1. P. DeShong, D. R. Sidler, P. J. Rybczynski, A. A. Ogilvie, and W. von Philipsborn, *J. Org. Chem.* **54,** 5432 (1989).
2. M. Koller and W. von Philipsborn, *Organometallics*, **11,** 467 (1992).
3. M. Koller, Ph.D. Thesis, University of Zurich, Zurich, Switzerland, 1993.
4. V. Tedesco and W. von Philipsborn, *Organometallics*, **14,** 3600 (1995).
5. E. J. Meier, W. Kozminski, A. Linden, P. Lustenberger, and W. von Philipsborn, *Organometallics*, **15,** 2469 (1996).
6. H. Bönnemann, W. Brijoux, R. Brinkmann, W. Meurers, R. Mynott, W. von Philipsborn, and T. Egolf, *J. Organometallic Chem.*, **272,** 231 (1984).
7. R. Fornika, H. Görls, B. Seeman, and W. Leitner, *JCS Chem. Commun.*, 1479 (1995).
8. R. G. Parr and W. Yang, *Density Functional Theory of Atoms and Molecules*, Academic Press, Oxford, UK, 1989.
9. J. M. Seminario and P. Politzer, Eds., *Modern Density Functional Theory*, Elsevier, Amsterdam, 1995.
10. T. Ziegler, *Can. J. Chem.*, **73,** 743 (1995).
11. V. G. Malkin, O. M. Malkina, M. E. Casida, and D. R. Salahub, *J. Am. Chem. Soc.*, **116,** 5898 (1994).
12. M. Kaupp, V. G. Malkin, O. L. Malkina, and D. R. Salahub, *Chem. Phys. Lett.*, **235,** 382 (1995).
13. M. Kaupp, V. G. Malkin, O. L. Malkina, and D. R. Salahub, *J. Am. Chem. Soc.*, **117,** 1851 (1995).
14. M. Kaupp, V. G. Malkin, O. L. Malkina, and D. R. Salahub, *Chem. Eur. J.*, **2,** 24 (1996).
15. M. Kaupp, *Chem. Eur. J.*, **2,** 194 (1996).
16. M. Kaupp, *Chem. Ber.*, **129,** 527 (1996).
17. M. Kaupp, *JCS Chem. Commun.*, 1141 (1996).
18. Y. Ruiz-Morales, G. Schreckenbach, and T. Ziegler, *J. Phys. Chem.*, **100,** 3359 (1996).
19. M. Bühl, O. L. Malkina, and V. G. Malkin, *Helv. Chim. Acta*, **79,** 742 (1996).
20. M. Bühl, *Organometallics*, **16,** 261 (1997).
21. M. Bühl, *Chem. Phys. Lett.*, **267,** 251 (1997).
22. B. Cornils and W. A. Herrmann, Eds., *Applied Homogeneous Catalysis with Organometallic Compounds, Vols. 1, 2*, VCH, Weinheim, 1996.
23. F. J. Feher and R. L. Blanski, *Organometallics*, **12,** 958 (1993).
24. F. J. Feher and R. L. Blanski, *J. Am. Chem. Soc.*, **114,** 5886 (1992).
25. A. D. Becke, *Phys. Rev. A*, **38,** 3098 (1988).
26. J. P. Perdew, *Phys. Rev. B*, **33,** 8822 (1986); *Phys. Rev. B*, **34,** 7046 (1986).
27. A. J. H. Wachters, *J. Chem. Phys.*, **52,** 1033 (1970).
28. P. J. Hay, *J. Chem. Phys.*, **66,** 4377 (1977).
29. C. Gonzales and H. B. Schlegel, *J. Chem. Phys.*, **90,** 2154 (1989); *J. Phys. Chem.*, **94,** 5523 (1990).
30. M. J. Frisch, G. W. Trucks, H. B. Schlegel, P. M. W. Gill, B. G. Johnson, M. A. Robb, J. R. Cheeseman, T. Keith, G. A. Petersson, J. A. Montgomery, K. Raghavachari, M. A. Al-Laham, V. G. Zakrzewski, J. V. Ortiz, J. B. Foresman, C. Y. Peng, P. Y. Ayala, W. Chen, M. W. Wong, J. L. Andres, E. S. Replogle, R. Gomperts, R. L. Martin, D. J. Fox, J. S. Binkley, D. J. DeFrees, J. Baker, J. J. P. Stewart, M. Head-Gordon, C. Gonzales, and J. A. Pople, *Gaussian-94*, Gaussian Inc., Pittsburgh, PA, 1995.
31. J. R. Cheeseman, G. W. Trucks, T. A. Keith, and M. J. Frisch, *J. Chem. Phys.*, **104,** 5497 (1996).
32. A. D. Becke, *J. Chem. Phys.*, **98,** 5648 (1993).
33. C. Lee, W. Yang, and R. G. Parr, *Phys. Rev. B*, **37,** 785 (1988).
34. S. Huzinaga and M. Klobukowski, *J. Mol. Struct.*, **167,** 1 (1988).
35. W. Kutzelnigg, U. Fleischer, and M. Schindler, In *NMR Basic Principles and Progress, Vol. 23*, Springer, Berlin, 1990, p. 167.
36. V. G. Malkin, O. L. Malkina, L. A. Eriksson, and D. R. Salahub, In *Modern Density Functional Chemistry*, J. M. Seminario and P. Politzer, Eds., Elsevier, Amsterdam, 1995, pp. 273–347.
37. D. R. Salahub, R. Fournier, P. Mlynarski, I. Papai, A. St-Amant, and J. Ushio, In *Density Functional Methods in Chemistry*, J. K. Labanowski and J. W. Andzelm, Eds., Springer, New York, 1991, p. 77.
38. A. St-Amant and D. R. Salahub, *Chem. Phys. Lett.*, **169,** 387 (1990).
39. J. J. Perdew, In *Electronic Structure of Solids*, P. Ziesche and H. Eischrig, Eds., Akademie, Berlin, 1991.
40. J. P. Perdew and Y. Wang, *Phys. Rev. B*, **45,** 13244 (1992).
41. K. Karakida and K. Kuchitsu, *Inorg. Chim. Acta*, **13,** 113 (1975).
42. H. Oberhammer and J. Strähle, *Z. Naturforsch.*, **30a,** 296 (1975).
43. A. Almenningen, S. Samdal, and D. Christen, *J. Mol. Struct.*, **48,** 69 (1978).
44. K. Hagen, M. M. Gilbert, L. Hedberg, and K. Hedberg, *Inorg. Chem.*, **21,** 2690 (1982).
45. D. C. Crans, H. Chen, D. P. Anderson, and M. M. Miller, *J. Am. Chem. Soc.*, **115,** 6769 (1993).
46. G. Doyle, K. A. Eriksen, and D. Van Engen, *Organometallics*, **4,** 2201 (1985).
47. e.g.: M. R. Bray, R. J. Deeth, V. J. Paget, and P. D. Sheen, *Int. J. Quantum Chem.*, **61,** 85 (1996).
48. O. W. Howarth, *Prog. NMR Spectrosc.*, **22,** 453 (1990).

49. D. Rehder, In *Transition Metal Nuclear Magnetic Resonance*, P. S. Pregosin, Ed., Elsevier, Amsterdam, 1991, p. 1.

50. A very small net deshielding is computed at pure DFT levels in going from **16** to **20** (Table II).

51. See, for example, the X-ray structure with an additional water molecule loosely attached to the vanadium atom: H. Rieskamp and R. Mattes, *Z. Naturforsch.*, **31b,** 541 (1976).

52. e.g.: H. Weiss, M. Ehrig, and R. Ahlrichs, *J. Am. Chem. Soc.*, **116,** 4919 (1994).

53. R. J. Meier, G. H. J. von Doremaele, S. Iarlori, and F. Buda, *J. Am. Chem. Soc.*, **116,** 7274 (1994).

54. T. Yoshida, N. Koga, and K. Morokuma, *Organometallics*, **14,** 746 (1995).

55. J. C. W. Lohrenz, T. K. Woo, L. Fan, and T. Ziegler, *J. Organometallic Chem.*, **497,** 91 (1995).

56. At the unrestricted BP86/I level, the V—O bond dissociation energy in **14** is ca. 106 kcal/mol, whereas that of the V—C bond in **13** is ca. 65 kcal/mol. See also the bond strengths in diatomic VO and VC, 149 and 112 kcal/mol, respectively: R. C. Weast, Ed., *CRC Handbook of Chemistry and Physics, 67th Edition*, CRC Press, Boca Raton, FL, 1986.